Available online at www.sciencedirect.com
SCIENCE DIRECT®
Composites Science and Technology 66 (2006) 2126–2134
COMPOSITES SCIENCE AND TECHNOLOGY
www.elsevier.com/locate/compscitech

# Modeling the compressive properties of glass fiber reinforced epoxy foam using the analysis of variance approach

M.V. Alonso *, M.L. Auad, S.R. Nutt [1]

*Gill Foundation Composites Center, Materials Science Department, University of Southern California, 3651 Watt Way, VHE-602 Los Angeles, CA 90089-0241, USA*

Received 20 July 2005; received in revised form 15 December 2005; accepted 22 December 2005
Available online 14 February 2006

**Abstract**

The aim of this work is to develop a (statistical) predictive model that describes the compression properties of glass-fiber-reinforced epoxy foams. An analysis of variance was applied in order to determine the behavior of the composite foams. The material variables and ranges used in the study were density (250–550 kg/m$^3$), fiber weight fraction (1–5 wt%), and fiber length (6–12 mm). The responses analyzed were the compressive modulus and strength. In addition, the foam size cell distribution was studied as a function of density. The results showed that the density and the morphology of composite foams exhibit a strong influence on the responses of the model. Therefore, the utilization of a statistical model for predicting composite foam properties is an appropriate tool that affords a global perspective of the influence of different effects on material behavior.


*Keywords:* A. Foam; A. Glass fibres; B. Mechanical properties; C. Statistical analysis

## 1. Introduction

Epoxy foams exhibit excellent mechanical properties and low shrinkage, low density, and low water absorption, all of which are especially attractive for applications in transportation and construction industries [1–4]. In recent years, these cellular materials have been improved by the incorporation of fillers such as fibers and particles [5–8]. The final properties of these cellular solids depend on foam density, the type and loading of fibers or particles, fiber length or particle diameter, and the geometrical structure of cells. It is a formidable but necessary task to link the physical properties of polymeric foams to the density and complex microstructure in order to understand and optimize such properties.

Considerable effort has been devoted to determining the behavior of polymeric foams through different models. One of the simplest approaches is to employ dimensional analysis. In this method, the mechanical properties of cellular materials are analyzed and predicted by considering the influence of relative density but not cell geometry [9]. For instance, Mourtiz [10] based his work on analytical models that predict post-fire mechanical properties of burnt composites. The author correlated different operating conditions of fire with flexure, tensile, and compressive properties of burnt specimens. Zhang and Chen [11] utilized a similar type of model to study the relation between low-cycle fatigue life of discontinuously reinforced metal matrix composites and the reinforced particle size.

Several authors have studied the mechanical performance of foams as a function of cell irregularity [12,13]. This method is based on analyzing a repeating unit cell,

* Corresponding author. Present address: Departamento de Ingeniería Química, Facultad de Ciencias Químicas, Universidad Complutense de Madrid, Avda de la Complutense s/n, 28040 Madrid, Spain. Tel.: +34 91 394 4240; fax: +34 91 394 4243.
*E-mail addresses:* valonso@quim.ucm.es (M.V. Alonso), nutt@usc.edu (S.R. Nutt).
[1] Tel.: +1 213 740 1634; fax: +1 213 740 7744.

0266-3538/$ - see front matter © 2006 Elsevier Ltd. All rights reserved.
doi:10.1016/j.compscitech.2005.12.016

**Nomenclature**

| | | | |
|---|---|---|---|
| $a_{ij}$ | regression coefficient | SDQ | sum of squares |
| $A$ | constant | $W$ | fiber weight fraction (wt%) |
| $B$ | constant | $X_{ij}$ | effect |
| df | degrees of freedom | $Z$ | response of the model |
| $E$ | compressive modulus (MPa) | | |
| $L$ | fiber length (mm) | *Greeks* | |
| $n$ | density exponent (Eq. (3)) | $\rho$ | density (kg/m$^3$) |
| $p$ | density exponent (Eq. (4)) | $\sigma_c$ | compressive strength (MPa) |

such as a tetrakaidecahedron. The mathematical tool utilized, in general, is finite elements. The random Voronoi technique followed by finite element analysis (FEA) improves the model accuracy and utility, because it provides a more accurate representation of the cell geometry of polymeric foams [14,15].

Another approach to modeling the behavior of cellular materials involves statistical methods. This approach reduces the number of experimental iterations and at the same time yields the maximum information about the different variables influencing the whole system. Using this approach, Sutherland and Soares [16] employed an experimental design to study the effect of energy absorbed by the specimen, clamp form, grip, and striker head on the impact response of glass-fiber-reinforced plastic. Similarly, Davim et al. [17] studied the influence of cutting parameters on the machining force in the workpiece, delamination factor, surface roughness, and international dimensional precision. In their work, they applied an orthogonal array $2^4$ experimental design. Such methods have proven to be useful and expeditious because of the increased efficiency coupled with acceptable accuracy.

The aim of this work is to determine the relationship between composition, final morphology, density, and properties of epoxy foams. A statistical model was utilized to describe the behavior of glass-reinforced epoxy foams when length, weight fraction, and density are changed in the selected ranges.

## 2. Experimental

### 2.1. Materials and synthesis of composite foams

Epoxy foams were formulated using a commercial system consisting of epoxy, amino hardener and polydimethylsiloxane as the chemical foaming agent (REN 1774, Ciba-Geigy, K.R. Anderson, USA). The epoxy foam was synthesized with an epoxy-to-hardener-to-blowing agent ratio of 100:25:1–4 (by weight). Short glass fibers were used with chop lengths of 6, 9, and 12 mm and an average diameter of 11 μm (Lauscha Fiber International). A silane sizing had been applied to the surface of the fibers.

The synthesis of reinforced epoxy foams was carried out by blending the resin and the fibers in a high-speed, dual-axis mixer (Keyence HM-101). After mixing, the hardener and the siloxane were incorporated into the mixture. The sample then was poured into a mold and maintained for 24 h at room temperature to expand the foam. Foam expansion was followed by post-curing for 2 h at 100 °C.

### 2.2. Statistical experimental design

Experimental design is an useful mathematical tool which yields a maximum of information for a minimum investment of experimental resources. In this work, only a brief description of statistical analysis of experimental design data is presented. More detailed information is provided elsewhere [18,19].

The aim of statistical design is to predict the behavior of a system or to optimize a process, and the first task is to develop or choose a model. Therefore, it is necessary to know the independent variables and dependent variables that study for choosing an appropriate model. The next step is to decide which factors (or independent variables) to analyze and to specify the ranges (“maximum” and “minimum” value from ranges or levels). In the present work, a full factorial design was chosen to describe the system, designated by $2^3$. This designation signifies that the experimental design has two levels with three independent variables (called factors). The levels are designated as “high” and “low” or “+1” and “−1”, respectively. A $2^3$ design was chosen because the availability of different glass fiber lengths was limited, as was the range of lengths suitable for foam production. A design with all possible high/low combinations from the range of the three factors led to the experiments summarized in Table 1. The ranges of the three factors considered in the $2^3$ design can be represented in a 3D space, as shown in Fig. 1. Each one of the numbers from the “*cube*” represents an iteration of the experimental design. In this work, three additional experiments were also preformed, and these runs correspond to the midpoints of the ranges studied for the independent variables. The iterations of the central point of the experimental design may be used as an estimate of the experimental variation [18]. The responses or the dependent variables of the system are influenced by the factors and the interactions between these (in the present case, the density, fiber length and fiber weight fraction).

Table 1
Matrix of two level full factorial design with three central points

| Run | Factor 1 | Factor 2 | Factor 3 |
|---|---|---|---|
| 1 | 0.0 | 0.0 | 0.0 |
| 2 | −1.0 | −1.0 | −1.0 |
| 3 | 1.0 | −1.0 | −1.0 |
| 4 | −1.0 | 1.0 | −1.0 |
| 5 | 1.0 | 1.0 | −1.0 |
| 6 | 0.0 | 0.0 | 0.0 |
| 7 | −1.0 | −1.0 | 1.0 |
| 8 | 1.0 | −1.0 | 1.0 |
| 9 | −1.0 | 1.0 | 1.0 |
| 10 | 1.0 | 1.0 | 1.0 |
| 11 | 0.0 | 0.0 | 0.0 |

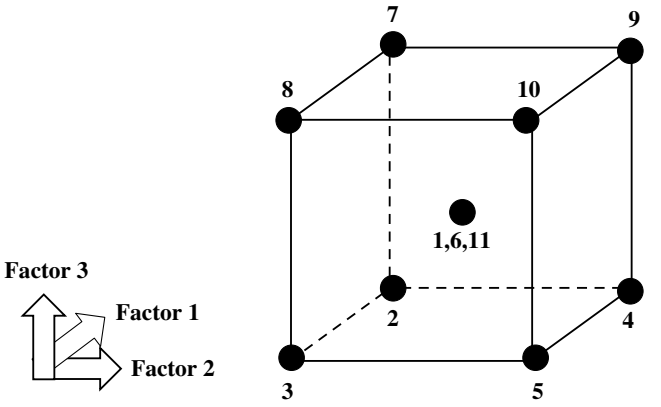


Fig. 1. Experimental design point according to two level full factorial design and three central points.

Experimental designs are employed to fit a linear statistical model to the response results, with factor levels coded as "low" or "high" for each factor. Currently, statistical software packages or spreadsheets allow calculating analysis of variance (ANOVA) and multiple linear regression methods. Thus, an example of a statistical model that can be obtained by $2^3$ designs is given by

$$Z = a_0 + \sum_{i=1}^{3} a_i X_i + \sum_{i=1}^{3} \sum_{j=1}^{3} a_{ij} X_i X_j, \tag{1}$$

where $Z$ is the response considered, $a_{ij}$ are the regression coefficients, and $X_{ij}$ are the effects studied. Once the regression coefficients are determined, an estimation or validation of the results is performed. Thus, each effect yields a *P-value*, which signifies the *significance* of that effect, either low or high. For instance, a higher *P-value* (>0.05%) indicates that the effect should be rejected in the variance analysis, because the effect lacks significance in the model. In addition, for determining the fit of the model, the data must show a low scatter and an $R^2$ value (fraction of the variance) near 100%. The responses can be plotted as a contour map or response surface (2D and/or 3D plot). In this manner, the graphs offer a visual analysis of the evolution of several factors that influence the response studied, which allows one to optimize the conditions of the system within the ranges considered.

### 2.3. Plan of experiments

The experimental work was divided in two parts. In the first part, six epoxy foams with densities between 250 and 550 kg/m$^3$ were formulated for determining the dependence of density on siloxane. These experiments determined the siloxane amount required for each iteration of the experimental design. In addition, compression tests and scanning electron microscopy (SEM) inspection were performed on these specimens. Data from the compression tests were analyzed using the Gibson–Ashby model [9]. The cell size distribution for each composite was determined from the SEM images.

In the second part of the work, a factorial design was followed to study the effects of the main variables on the manufacture of glass-fiber-reinforced epoxy foams. A $2^3$ central composite design was applied (11 runs: $2^3 + 3$ center points), which included three main effects and three two-factor interactions. The variables studied were density ($\rho$), fiber weight fraction ($W$), and fiber length ($L$), and the respective ranges were 250–550 kg/m$^3$ (or 15.4–34 pcf), 1–5 wt%, and 6–12 mm. The responses measured for model development were modulus ($E$) and compressive strength ($\sigma_c$).

The experimental conditions employed and the results obtained are shown in Table 2. Data processing was accomplished using commercial software (*Statgraphics plus*®5.0). The model equations included first-order terms to describe main effects, and second-order terms for interactions, as

$$Z = a_0 + a_\rho \rho + a_L L + a_W W + \alpha_{\rho L} \rho L + a_{\rho W} \rho W + a_{WL} WL. \tag{2}$$

Analysis of variance for experimental results was employed to discount non-significant effects, which were excluded from the model regression, and to check the suitability of the model. Contour maps (three- and two-dimensional response surfaces) from the model were employed to locate the optimum conditions of the process.

Table 2
The design of experiment generated matrix, along with the compression test results

| Run | Density (kg/m$^3$) | Length (mm) | Loading (wt%) | Modulus (MPa) | Strength (MPa) |
|---|---|---|---|---|---|
| 1 | 250 | 6 | 1 | 39.96 | 2.27 |
| 2 | 250 | 12 | 1 | 62.25 | 1.96 |
| 3 | 550 | 12 | 5 | 183.48 | 16.65 |
| 4 | 550 | 6 | 5 | 200.20 | 16.47 |
| 5 | 550 | 6 | 1 | 149.33 | 19.55 |
| 6 | 400 | 9 | 3 | 79.90 | 4.67 |
| 7 | 550 | 12 | 1 | 132.55 | 17.76 |
| 8 | 400 | 9 | 3 | 80.30 | 4.72 |
| 9 | 250 | 12 | 5 | 62.94 | 3.46 |
| 10 | 400 | 9 | 3 | 79.80 | 4.69 |
| 11 | 250 | 6 | 5 | 40.85 | 2.85 |

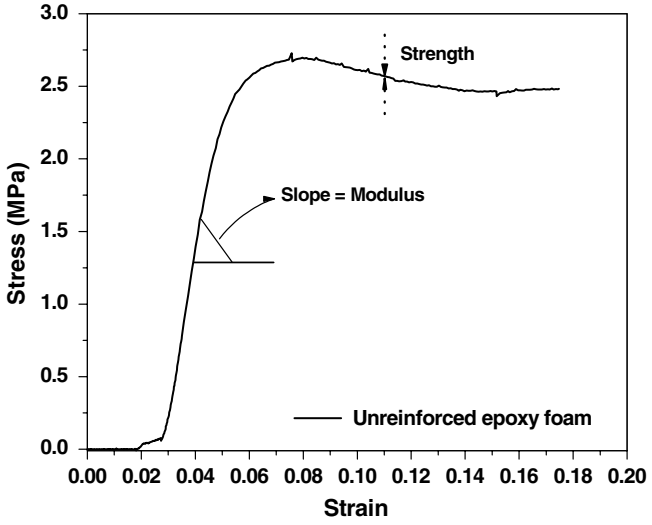


Fig. 2. Compressive stress–strain curve of epoxy foam. Loading direction is parallel to the foam rise direction.

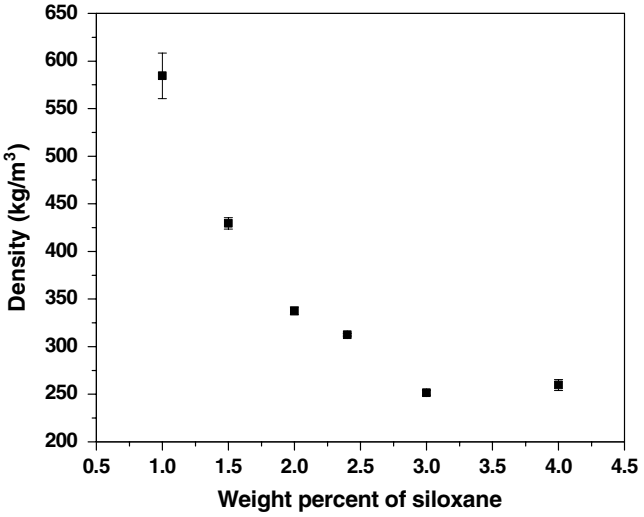


Fig. 3. Variation of the density with the weight percent siloxane for unreinforced epoxy foams.

### 2.4. Compression tests

Compression testing was performed on a universal testing machine (INSTRON 8531) in accordance with ASTM D1621. Specimens were cut with a diamond blade band saw and polished to obtain dimensions of 30 $mm^2$ by 25.4 mm thick. The samples were placed between stainless steel platens and load was applied with a crosshead rate of 2.5 mm/min. Compressive modulus was determined from the steepest initial slope of the stress–strain curve and strength was calculated from the maximum load (in a range of strain <10%), as shown in Fig. 2. Average values were determined from a minimum of five replicates.

### 2.5. Scanning electron microscopy

A scanning electron microscope (SEM, Cambridge 360) was employed to observe the surfaces of foam specimens. Samples were prepared by cryogenic fracture, which produced a viewable cross-section perpendicular to the rise direction to avoid structural deformation of the foams. Gold sputtering onto the sample surface was used to impart electrical conductivity. The operation voltage of the SEM was 10 kV.

## 3. Results and discussion

### 3.1. Characterization of unreinforced and reinforced epoxy foams

The density of the epoxy-amine foam system decreased sharply as the amount of blowing agent, siloxane, was increased from 1 to 4 wt%, as shown in Fig. 3. During the foaming process, the blowing agent reacts with the amine producing hydrogen gas, which results in foam expansion. However, the density remains constant and does not decrease when 3 wt% or more siloxane is added. In fact, higher siloxane contents (>3 wt%) produced a collapse of cells, as shown in Fig. 4. Thus, formulation of the epoxy-amine system with a ratio of 100:25 was carried out with blowing agent contents less than 3 wt%. Therefore, the range limits of the blowing agent content for the experimental design application were set at 1 and 3 wt% siloxane.

The compressive modulus ($E$) and compressive strength ($\sigma_c$) are plotted as functions of foam density in Figs. 5 and 6, respectively. Both mechanical properties increase substantially with foam density (which is controlled by the amount of blowing agent). The compressive modulus and strength can be fitted to a power-law expression with respect to foam density [20], as follows:

$$E = A\rho^n, \tag{3}$$

$$\sigma_c = B\rho^p, \tag{4}$$

where $A$ and $B$ are constants related to the physical properties of the foams, and $n$ and $p$ are density exponents related to the structure and deformation mechanics of the cellular material. Although Eqs. (3) and (4) were originally proposed by Gibson and Ashby for open-cell foams, several authors have applied them to closed-cell foams [20,21]. The compressive modulus and strength data in the density range studied is accurately described by the equations. The fits results of Figs. 5 and 6 are 0.98 and 0.97, respectively. The values obtained for the parameters "$n$" and "$p$" were 1.6 and 2.2, respectively, and are consistent with recent reports for similar composite foams [9,21].

These results indicate that the morphology of epoxy foam changes as a function of density according to Eqs. (3) and (4). Accordingly, SEM samples were prepared to determine *how* the cell size distribution changed with foam density. Fig. 7 shows typical SEM images of the cell size distributions in foams with different amounts of siloxane.

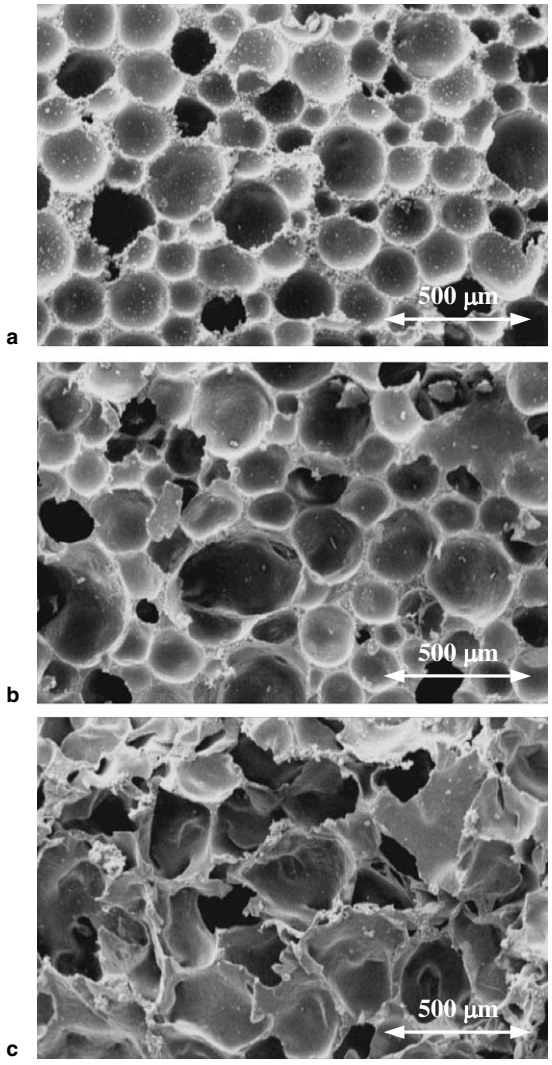


Fig. 4. SEM images of unreinforced epoxy foams: (a) 1 wt% siloxane, (b) 2.5 wt% siloxane, and (c) 4 wt% siloxane.

Cell sizes measured from such images are plotted in Fig. 7(d), which shows that the distribution of cell sizes was displaced to higher diameters when the siloxane content was increased. The average cell diameters increase from 0.105 to 0.16 mm when the blowing agent is increased from 1 to 3 wt%.

The effect of different fiber weight fractions and fiber lengths on cell size distribution was considered in foams of fixed density. In recent work, it was reported that the cell size distribution was not significantly modified by different fiber loadings [22]. In the case of different fiber length, the cell size in reinforced epoxy foams was not significantly affected, as shown in Fig. 8. Thus, we conclude that size cell distribution was not significantly affected by glass fiber loading or fiber length. These findings provide an excellent opportunity to study glass-fiber-reinforced epoxy foams through statistical model, considering that the size distribution of cell does not change in foams of fixed density. The following section presents the results of an analysis of variance study (ANOVA) of reinforced epoxy foams.

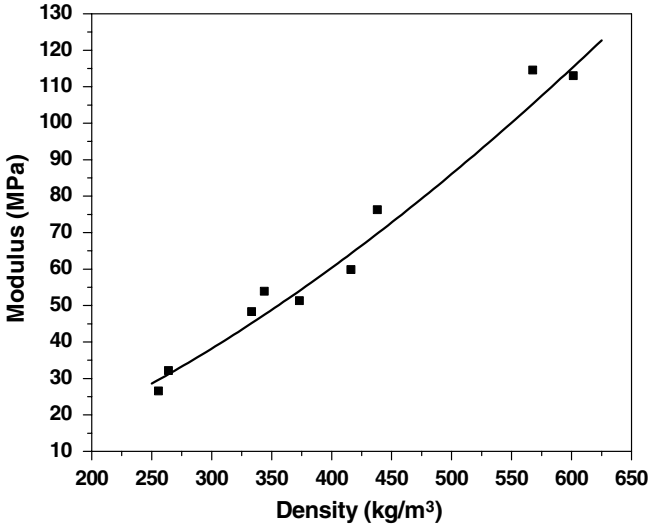


Fig. 5. Variation of the compression modulus with the density for unreinforced epoxy foams.

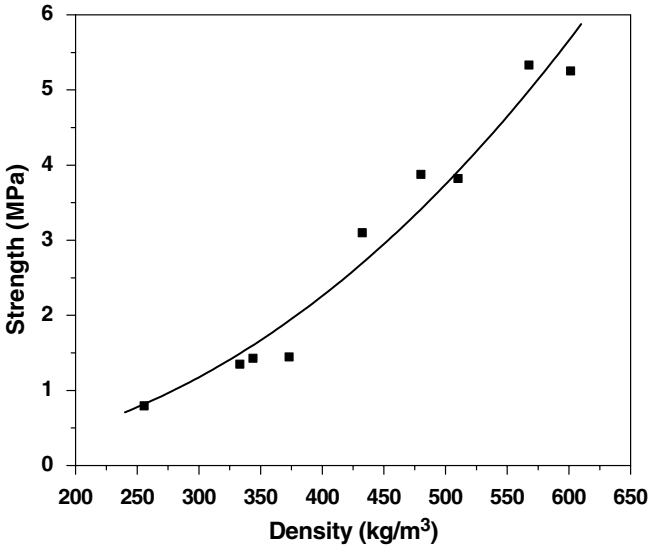


Fig. 6. Variation of the compression strength with the density for unreinforced epoxy foams.

### 3.2. Statistical model of reinforced epoxy foams

The measured values of compression modulus ($E$) and strength ($\sigma_c$) provided a basis for evaluating the behavior of the reinforced composite foams. The values of compressive modulus and strength are summarized in Table 2. Modulus and strength were increased up to ~40% and ~20%, respectively, when the amount and length of fibers added were optimized according to statistical model, as described below.

The influence of density ($\rho$), fiber length ($L$) and fiber weight fraction ($W$) was studied through statistical design. The analysis of variance (ANOVA) for modulus of reinforced epoxy foams is shown in Table 3. This analysis was carried out for a level of confidence of 95%. The last

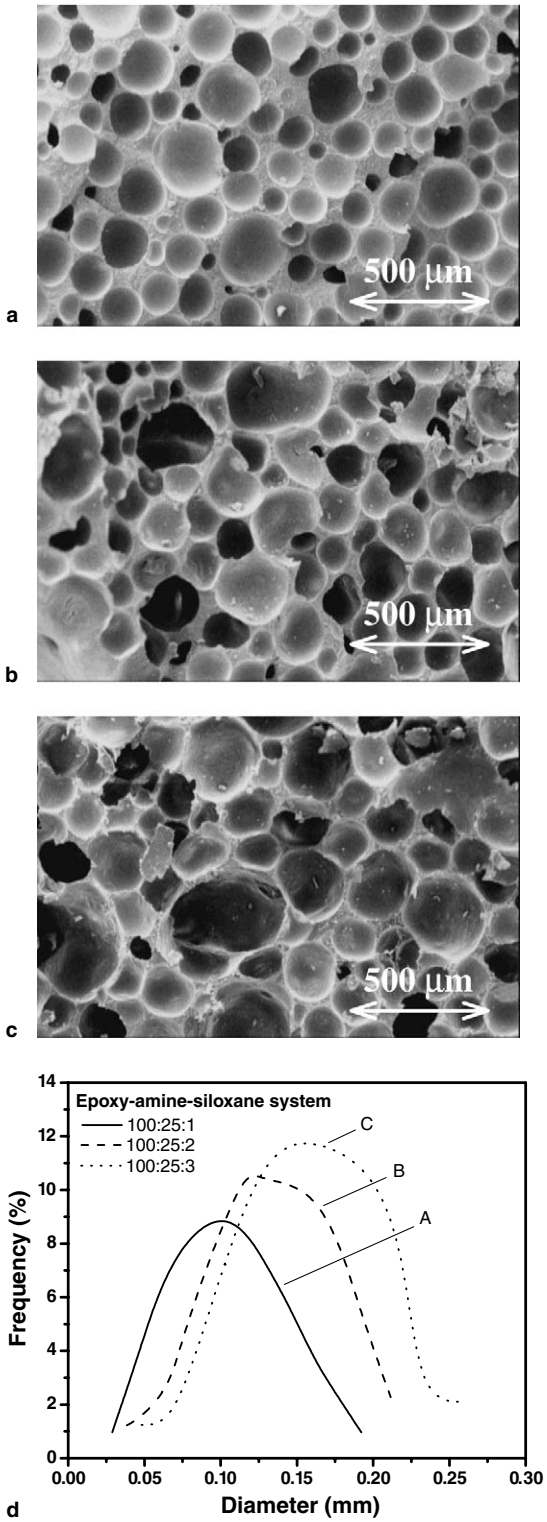


Fig. 7. SEM images of epoxy-amine foams with different amount of siloxane: (a) 100:25:1, (b) 100:25:2, and (c) 100:25:3. (d) Distribution of cell size for unreinforced epoxy foams (curve A, B and C correspond to epoxy-amine-siloxane system with a ratio of 100:25:1, 100:25:2 and 100:25:3, respectively).

two columns in Table 3 indicate the distribution $F$ and *P-values* of each factor and their influence on the analysis. The factors with a distribution $F > 18.58\%$ and *P-values* $< 0.05$ exhibit statistical significance level higher than 95% for compression modulus. However, in cases where the factor had a distribution $F < 18.58\%$ and *P-values* $> 0.05$, the factor or factors must be rejected because the effects present a significance level less than 95%. Thus, as shown in Table 3, the factor WL must be rejected from the analysis of variance. The new ANOVA values for the modulus are shown in Table 4. All factors display a confidence level of 95%. The corresponding revised model obtained describing the modulus for the composite foams (in the range studied), is given by

$$E\ (\mathrm{MPa}) = -103.371 + 0.452394 \cdot \rho + 9.10743 \cdot L - 10.2432 \cdot W - 0.0216347 \cdot \rho L + 0.0417604 \cdot \rho W. \quad (5)$$

The response surfaces of the modulus as a function of fiber weight fraction and fiber length are shown in Fig. 9(a)–(c), for a density of 250, 400, and 550 kg/m$^3$, respectively. The surface plots show that the effects of fiber weight fraction and fiber length affect the modulus differently when the density value is modified. For example,

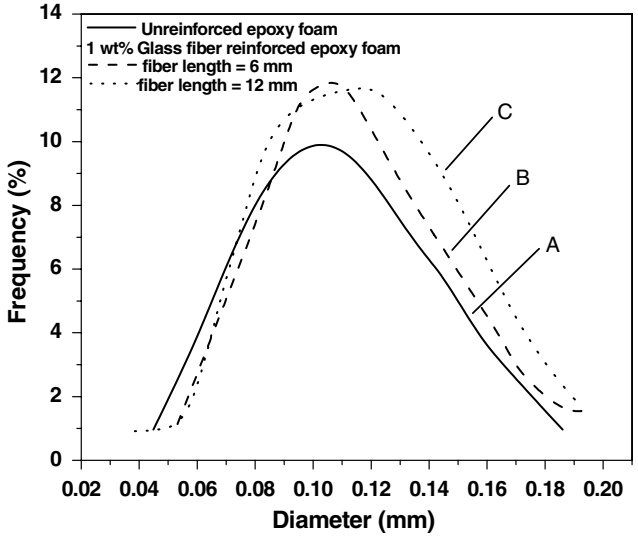


Fig. 8. Distribution of cell size for unreinforced and reinforced epoxy foam samples with 1 wt% siloxane. Curve A: unreinforced epoxy foam, Curve B: 1 wt% glass fiber reinforced epoxy foam, $l = 6$ mm, and Curve C: 1 wt% glass fiber reinforced epoxy foam, $l = 12$ mm.

Table 3
Analysis of variance for the compression modulus ($E$)

| Source | SDQ | Mean square | df | Test $F$ | *P-values* |
|---|---|---|---|---|---|
| $\rho$ | 26398.80 | 26398.80 | 1 | 377126.43 | 0.0000 |
| $W$ | 14.81 | 14.81 | 1 | 211.58 | 0.0047 |
| $L$ | 1335.80 | 1335.80 | 1 | 19082.84 | 0.0001 |
| $\rho W$ | 758.26 | 758.26 | 1 | 10832.27 | 0.0001 |
| $\rho L$ | 1255.63 | 1255.63 | 1 | 17937.59 | 0.0001 |
| $WL$ | 0.00263 | 0.00263 | 1 | 0.04 | 0.8643 |
| Lack of fit | 1828.04 | 914.022 | 2 | 13057.45 | 0.0001 |
| Error | 0.14 | 0.07 | 2 | – | – |
| Total | 31591.5 | – | 10 | – | – |

SDQ: sum of squares, df: degrees of freedom.

Table 4
Analysis of variance for the compression modulus ($E$) with all significance effects

| Source | SDQ | Mean square | df | Test $F$ | *P-values* |
|---|---|---|---|---|---|
| $\rho$ | 26398.80 | 26398.80 | 1 | 377126.43 | 0.0000 |
| $W$ | 14.81 | 14.81 | 1 | 211.58 | 0.0047 |
| $L$ | 1335.80 | 1335.80 | 1 | 19082.84 | 0.0001 |
| $\rho W$ | 758.26 | 758.26 | 1 | 10832.27 | 0.0001 |
| $\rho L$ | 1255.63 | 1255.63 | 1 | 17937.59 | 0.0001 |
| Lack of fit | 1828.04 | 609.35 | 3 | 8704.98 | 0.0001 |
| Error | 0.14 | 0.07 | 2 | – | – |
| Total | 31591.5 | – | 10 | – | – |

SDQ: sum of squares, df: degrees of freedom.

for composite foams of low density (250 kg/m$^3$), only fiber length exhibits a marked influence on the modulus (Fig. 9(a)). However, for intermediate density foams (~400 kg/m$^3$), the fiber weight fraction effects have a greater influence on modulus (Fig. 9(b)). And when the foam density is higher (550 kg/m$^3$), the influence of fiber length and fiber weight fraction on the modulus is greater still, as shown in Fig. 9(c). In this case, both effects exert similar influences on the composite foam modulus. On the other hand, the magnitude of the effect these factors have on foam modulus depends also on the foam density. Thus, the main effect that influences foam modulus is density, and the variation in cell morphology with density is the main cause. In addition, density produces a different response in modulus and consequently, the effect of fiber weight fraction and length change with the density.

The analysis of variance for compressive strength of glass-reinforced epoxy foams is shown in Table 5. The values of distribution $F$ and *P-values* for all factors are >18.58% and <0.05, respectively. Therefore, the factors present a significance level higher than 95% and no factor was rejected. The model obtained for compressive strength is expressed by

$$\sigma_c\ (\text{MPa}) = -13.8545 + 0.0625208 \cdot \rho - 0.0229861 \cdot L + 0.37125 \cdot W - 0.000530556 \cdot \rho L - 0.0026125 \cdot \rho W + 0.0602083 \cdot WL. \quad (6)$$

The response surface plots of compressive strength for two densities are shown in Fig. 10. The evolution of compressive strength with foam density, fiber weight fraction and fiber length displays behavior different than that of the modulus. The tendency of compressive strength can be defined for density values lower than 350 kg/m$^3$ and for densities $\geqslant$350 kg/m$^3$. In the first (low-density) regime, high values of fiber weight fraction and length are required to yield high compressive strength values. In the second (higher-density) regime, the response surface exhibits a "saddle" (Fig. 10(b)).

Details of the saddle are shown more clearly in the 2D contour map shown in Fig. 11. In this figure, high strength values are obtained when the composite epoxy foam contains a high fiber weight fraction with high fiber lengths, or a low fiber weight fraction and with low fiber lengths.

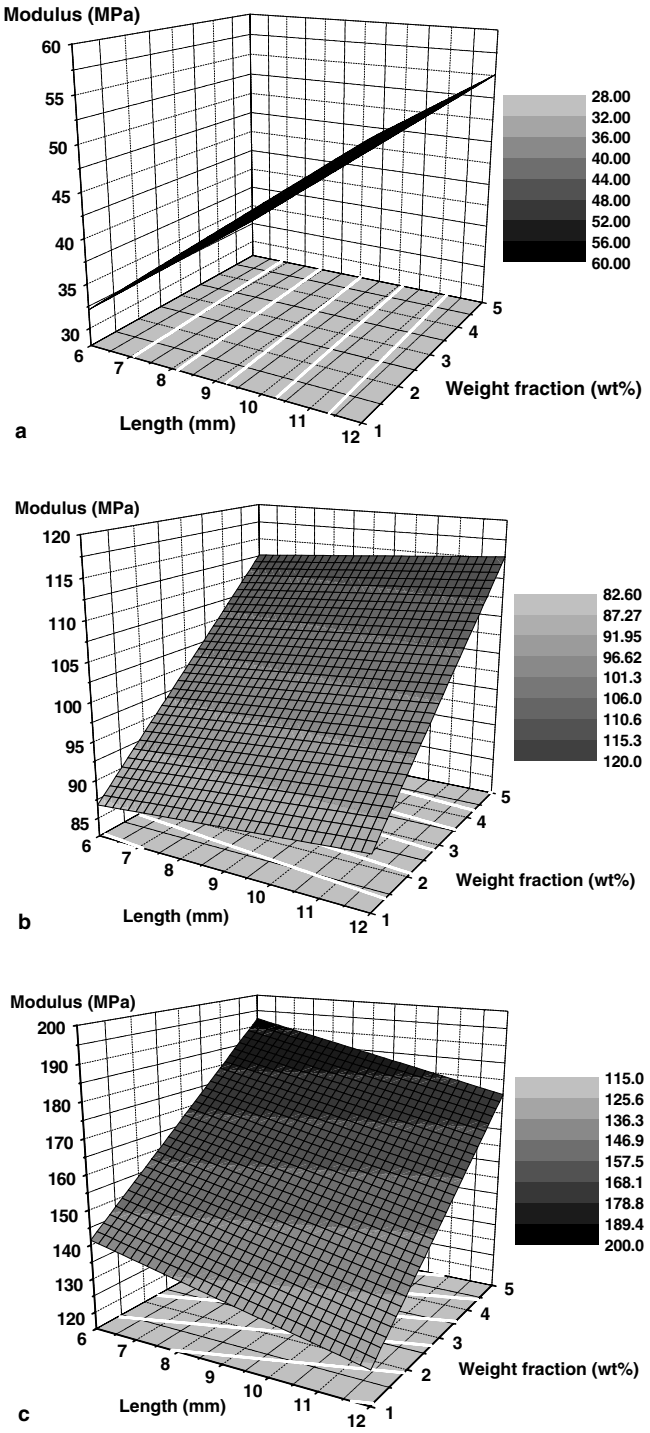


Fig. 9. The variation of compressive modulus with fiber length and fiber weight fraction: (a) foam density = 250 kg/m$^3$, (b) foam density = 400 kg/m$^3$, and (c) foam density = 550 kg/m$^3$.

This raises a question of why the strength decreases as one moves towards either of two corners of the surface (upper left or lower right), and whether or not this constitutes an artifact of the statistical model. Accordingly, two additional experiments were performed with glass fiber weight fractions of 1 and 2 wt% and fiber lengths of 9 and 12 mm, respectively, to produce composite foams of

Table 5
Analysis of variance for the compression strength ($\sigma_c$)

| Source | SDQ | Mean square | df | Test $F$ | *P-values* |
|---|---|---|---|---|---|
| $\rho$ | 448.352 | 448.352 | 1 | 854002.88 | 0.0000 |
| $W$ | 0.214 | 0.214 | 1 | 408.60 | 0.0024 |
| $L$ | 0.557 | 0.557 | 1 | 1060.02 | 0.0009 |
| $\rho W$ | 0.456 | 0.456 | 1 | 868.60 | 0.0011 |
| $\rho L$ | 4.914 | 4.914 | 1 | 9360.21 | 0.0001 |
| $WL$ | 1.044 | 1.044 | 1 | 1988.60 | 0.0005 |
| Lack-of-fit | 64.379 | 32.189 | 2 | 61313.98 | 0.0000 |
| Error | 0.00105 | 0.000525 | 2 | – | – |
| Total | 519.917 | – | 10 | – | – |

SDQ: sum of squares, df: degrees of freedom.

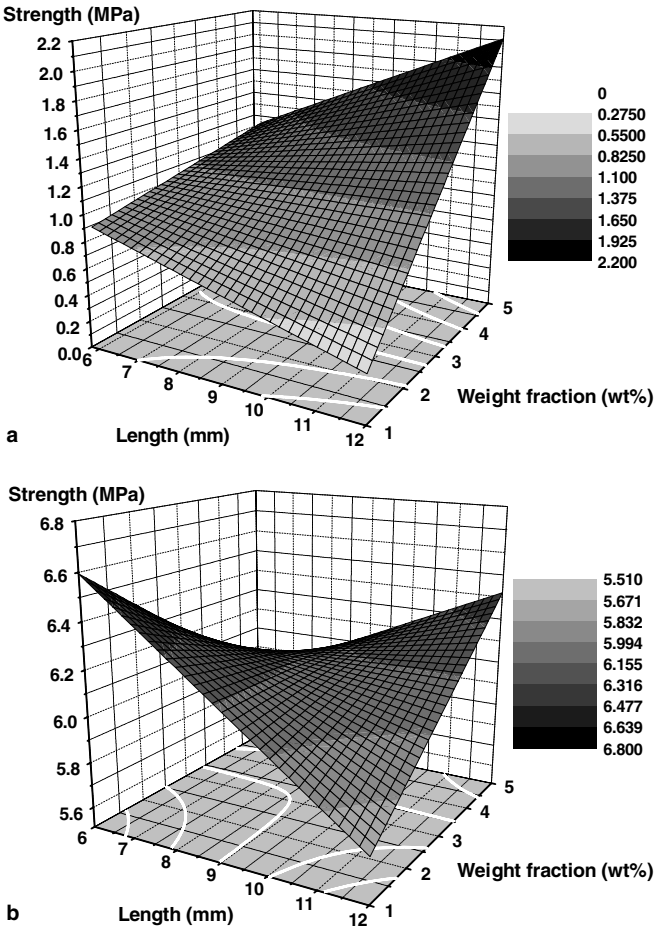


Fig. 10. The variation of compressive strength with fiber length and fiber weight fraction: (a) Foam density = 250 kg/m$^3$ and (b) foam density = 350 kg/m$^3$.

fixed density ($\rho = 350$ kg/m$^3$). These samples exhibited strength values of 5.54 and 5.23 MPa for 1 and 2 wt% glass fiber weight fractions, respectively. The values predicted for these samples are 6.14 and 5.51 MPa for 1 and 2 wt% glass fiber weight fractions, respectively. Therefore, the difference between the experimental value and the predicted value was ~10%, demonstrating the predictive accuracy of the proposed model and validating the prediction.

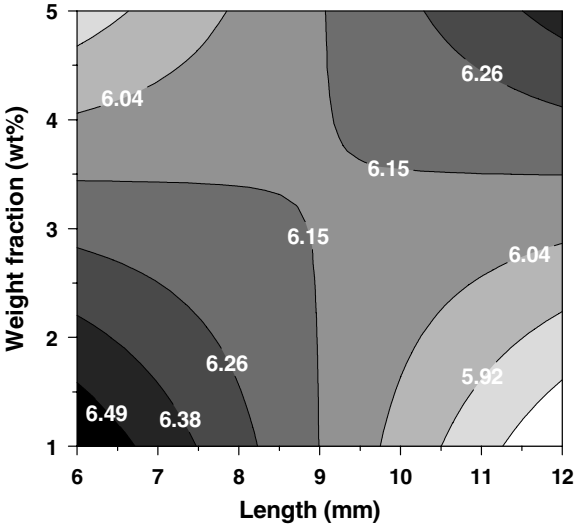


Fig. 11. Contour plot of the compression strength ($\rho = 350$ kg/m$^3$).

Understanding the evolution of compressive modulus and strength and the dependence on simple material parameters enables on to select process conditions to optimize mechanical performance required for the final application. For instance, epoxy foam reinforced with 5 wt% of glass fibers of length ~9 mm ($\rho = 350$ kg/m$^3$) will yield a compressive modulus and a strength of 90 and 6.2 MPa, respectively. These properties are competitive with commercially phenolic and polyurethane foams [23]. Thus, experimental design can be used as a predictive design tool and as an experimental aid to reduce the number of experiments required and to select optimized process parameters to yield the performance required by specific applications.

## 4. Conclusions

In the present work, an epoxy-amine system was used to produce structural foams, and the compression properties were well-described by a simple power law. However, composite foam systems are more complex, and a more powerful tool such as statistical design is required to predict mechanical performance. This tool was employed in the present study to investigate the effects of several simple and controllable variables on the properties of epoxy composite foams.

Although this work demonstrates the utility of this type of statistical design for optimizing the properties of reinforced epoxy foams, there is ample room for refinement of models to yield improved accuracy. Clearly, materials with characteristics similar to epoxy foams can be analyzed and optimized with statistical design to reduce the number of experiments and to predict the influence of several controllable effects on the properties. In the case of reinforced epoxy foams, it would useful to extend the method to more complex statistical designs. This could lead to a determination of the influence of multiple effects such as fiber type,

fiber aspect ratio, fiber orientation, and strength/stiffness ratio. In addition, the approach could be extended to determine the influence of these effects on other mechanical properties.

## Acknowledgments

The authors gratefully acknowledge the support of the Merwyn C. Gill Foundation. One of the authors also thanks the support of "Secretaría de Estado de Educación y Universidades" (from Spanish Government) and the co-support of "Fondo Social Europeo".

## References

[1] Kloker H, Gossen H, Winkler H. Schaumstoffe and Schaumstoff-Leichbeton auf Basus ungesattigter Polyesterresins. Kunststoffe 1970;60(8):555–8.
[2] Lee H, Neville K. Handbook of epoxy-resin. New York: McGraw-Hill; 1982.
[3] Moser A, Kamps E. Lverarbeitung und Anwendungen mit expandierenden EP-Harzen als Matrixsysteme. In: 21 AVK conference, Mainz, 1987. p. 32–4.
[4] Cole LF. Epoxy resins and polyurethane foams for low pressure injection crack repair. Concr Repair Bull 2000:8–10.
[5] Shen H, Nutt S. Mechanical characterization of short fiber reinforced phenolic foam. Compos Pt A: Appl Sci Manufact 2003;34:899–906.
[6] Vaikhanski L, Nutt SR. Fiber-reinforced composite foam from expandable PVC microspheres. Compos Pt A: Appl Sci Manufact 2003;34:1245–53.
[7] Carfagna C, Ambrogi V, Cicala G, Pollicino A, Recca A, Costa G. Reactive microspheres as active fillers for epoxy resins. J Appl Polym Sci 2004;93(5):2031–44.
[8] Savage G. Enhancing the exploitation and efficiency of fibre-reinforced composite structures by improvement of interlaminar fracture toughness. Eng Fail Anal 2006;13(2):198–209.
[9] Gibson LJ, Ashby MF. Cellular solids: structure and properties. Cambridge, UK: Cambridge University Press; 1997.
[10] Mouritz AP. Simple models for determining the mechanical properties of burnt FRP composites. Mater Eng A 2003;359:237–46.
[11] Zhang Q, Chen DL. A model for predicting the particle size dependence of the low cycle fatigue life in discontinuously reinforced MMCs. Scripta Mater 2004;51:863–7.
[12] Gibson LJ, Ashby MF. Cellular solids. Oxford: Pergamon Press; 1988.
[13] Kraynik AM, Warren WE. In: Hilyard NC, Cunningham A, editors. In low density cellular plastics. London: Chapman and Hall; 1994.
[14] Zhu HX, Hobdell JR, Windle AH. Effects of cell irregularity on the elastic properties of open-cell foams. Acta Mater 2000;48:4893–900.
[15] Zhu HX, Hobdell JR, Windle AH. Effects of cell irregularity on the elastic properties of 2D Voronoi honeycombs. J Mech Phys Solids 2001;49:857–70.
[16] Sutherland LS, Soares CG. The effects of test parameters on the impact response of glass reinforced plastic using an experimental design approach. Compos Sci Technol 2003;63:1–18.
[17] Davim JP, Reis P, Antonio CC. A study on milling of glass fiber reinforced plastics manufactured by hand-lay up using statistical analysis (ANOVA). Compos Struct 2004;64:493–500.
[18] Montgomery DC. Design and analysis of experiments. New York: Wiley and Sons, Inc.; 1991.
[19] Box GEP, Hunter WG, Hunter JS. Statistics for experimenters: an introduction to design, data analysis, and model building. New York: John Wiley and Sons; 1978.
[20] Goods SH, Neuschwanger CL, Whinnery LL, Nix WD. Mechanical properties of a particle-strengthened polyurethane foam. J Appl Polym Sci 1999;74(11):2436–724.
[21] Stefani PM, Barchi AT, Sabugal J, Vazquez A. Characterization of epoxy foams. J Appl Polym Sci 2003;90(11):2992–6.
[22] Alonso MV, Auad ML, Nutt SR. Short-fiber-reinforced epoxy foams. Compos Pt A: Appl Sci Manufact, in press.
[23] FR-4500® Series foam product, General Plastics manufacturing company, 2004.Alucopan® foam product, Alcan Aires AG Company, 2003.